TRANSACTIONS ON ELECTRICAL AND ELECTRONIC MATERIALS
Vol. 18, No. 1, pp. 7-12, February 25, 2017

Regular Paper

pISSN: 1229-7607 eISSN: 2092-7592
DOI: https://doi.org/10.4313/TEEM.2017.18.1.7
OAK Central: http://central.oak.go.kr

# Effect of Boron Content and Temperature on Interactions and Electron Transport in BGaN Bulk Ternary Nitride Semiconductors

Yasmina Bouchefra† and Nasr-Eddine Chabane Sari
*Unity of Research Materials and Renewable Energies (URMER), University of Tlemcen, Chetouane 13000, Algeria*

**Received March 17, 2016; Revised August 17, 2016; Accepted September 21, 2016**

This work takes place in the context of the development of a transport phenomena simulation based on group III nitrides. Gallium and boron nitrides (GaN and BN) are both materials with interesting physical properties; they have a direct band gap and are relatively large compared to other semiconductors. The main objective of this paper is to study the effect of boron content on the electron transport of the ternary compound $B_xGa_{(1-x)}N$ and the effect of the temperature of this alloy at x=50% boron percentage, specifically the piezoelectric, acoustic, and polar optical scatterings as a function of the energy, and the electron energy and drift velocity versus the applied electric field for different boron compositions ($B_xGa_{(1-x)}N$), at various temperatures for $B_{0.5}Ga_{0.5}N$. Monte carlo simulation, was employed and the three valleys of the conduction band (Γ, L, X) were considered to be non-parabolic. We focus on the interactions that do not significantly affect the behavior of the electron. Nevertheless, they are introduced to obtain a quantitative description of the electronic dynamics. We find that the form of the velocity-field characteristic changes substantially when the temperature is increased, and a remarkable effect is observed from the boron content in $B_xGa_{(1-x)}N$ alloy and the applied field on the dynamics of holders within the lattice as a result of interaction mechanisms.

**Keywords:** $B_xGa_{(1-x)}N$, Monte carlo simulation, Boron content, Temperature, Scattering rates, Electron energy, Drift velocity

## 1. INTRODUCTION

The majority of the III-nitride compounds are large band gap semiconductors, which makes them excellent candidates for optoelectronics [1]. Indeed, the incorporation of boron in GaN material eliminates lattice parameter disagreement, forming a $B_xGa_{(1-x)}N$ alloy. This alloy possesses very advantageous physical properties such as high thermal conductivity, great robustness, excellent thermal stability and optical transparency in a very important spectral range, which make them very attractive for many applications.

Transport phenomena in this semiconductor result from the behavior of electrons in the conduction band and energy gap. The Knowledge of the electron energy distribution function is obtained from the resolution of the partial derivative Boltzmann equation [2], which makes it possible to study the transport phenomena in semiconductor materials. Nevertheless, the analytical solution for this equation is very complex, and often requires digital simulations. Simulation by the Monte carlo method is one of these techniques, and makes it possible to accurately reproduce the various microscopic phenomena that exist in semiconductor materials [3].The advantage of Monte carlo's method is that it obtains both the duration of free-flight [4], and the carrier states after collisions using a process based on drawing random numbers, on one side, and knowledge of the probability densities that correspond to the interactions to which the carrier is subjected on the other. Hence, a FORTRAN program based on this method has been developed [5,6]. It enables the calculation of probabilities from the standard expressions. In our case, we consider a model with three valleys

† Author to whom all correspondence should be addressed:
E-mail: bouchefra_yasmina@yahoo.fr

(Γ, L, X) [7], isotropic but not parabolic, in order to determine the evolution of the scattering, electronic energy and drift velocity in the ternary material $B_xGa_{(1-x)}N$ for different boron compositions at x=50% for different temperatures.

## 2. MODEL DETAILS

The use of a Monte carlo method is well suited for semiconductor electron transport simulation. It is a statistical method and an effective mathematical tool for the study and analysis of the physical phenomena. Several works have contributed to the improvement and development of the Monte carlo method such as those of Price [8], Hockney [9], and Jacoboni et al [10], who studied the model for several bands. In general terms, the method is based on a drawing of lots for the interactions experienced by carriers during their movements within the crystal lattice using probability laws. It follows the behavior of each electron subjected to an electric field $\vec{E}$ in real space and in the waves vectors space [11]. Let us consider for each carrier, an initial wave vector $\vec{k}_0$ and an initial vector position $\vec{r}_0$, for which we want to simulate the trajectory. Using the "self-scattering" procedure, we introduce a fictitious scattering that creates a distribution of time. With each simulated electron "p", we associate an initial wave vector $\vec{k}$ with an initial position $\vec{r}$.

$$\vec{k}_p(t),\vec{r}_p(t)\vec{E}_p(t)=\vec{E}(\vec{k}_p) \tag{1}$$

We are performing a coasting flight with duration t, so we will have:

$$\begin{cases}\vec{k}_p(t+\Delta t)=\vec{k}_p(t)+\dfrac{e\vec{E}}{\eta}\Delta t\\ \vec{E}_p(t+\Delta t)=\overrightarrow{E(k_p}(t+\Delta t))\\ \vec{r}_p(t+\Delta t)=\int\vec{V}_p(t)dt\end{cases} \tag{2}$$

If there is no interaction, we check whether the state of the carrier changes, and if there is an interaction, we check whether the interaction occurs precisely at the instant t+ Δ t. One seeks the new wave vector $\vec{k}_p^{'}$ after the collision by drawing lots from a random number. The state is now defined by:

$$\begin{cases}\vec{k}_p^{'}(t+\Delta t)\\ \vec{E}_p^{'}(t+\Delta t)=\vec{E}_p(\vec{k}_p^{'}(t+\Delta t))\\ \vec{r}_p^{'}(t+\Delta t)=\vec{r}_p(t+\Delta t)\end{cases} \tag{3}$$

The results obtained with the Monte carlo studies are strongly related to many physical parameters. Using the information obtained, analysis was performed based on the material parameters entered into the simulator. The results were compared with actual experimental results providing knowledge of the physical effects and their consequences in the material. The basic and band structure parameters of BN and GaN materials used in our simulation are given in table1.

Table 1. Basic parameters of BN and GaN materials.

| Parameters | | BN | GaN |
|---|---|---|---|
| Relative mass | r | 0.75 [12] | 0.15[15] |
| | L | 0.55 [12] | 0.60 [15] |
| | X | 0.30 [12] | 0.50 [15] |
| Energy (ev) | r | 9.94 [13] | 3.38 [15] |
| | L | 14.3 [13] | 5.64 [15] |
| | X | 12.04[13] | 4.57 [15] |
| High-frequency permittivity | | 4.5 [14] | 5.35 [16] |
| Low-frequency permittivity | | 7.1 [14] | 9.50 [16] |

## 3. MECHANISMS OF SCATTERINGS:

Scatterings are essential ingredients in all Monte carlo simulations. The statistical study of possible energy exchanges between electrons, the vibration modes of lattice vibrations and impurities, allows for the calculation of the probability of these scatterings and their effect on energy as well as the wave vector of the electron. The scattering considered in this work, mainly due to acoustic, piezoelectric and polar optical phonons, are applied to $B_xGa_{(1-x)}N$ for different boron compositions and to $B_{0.5}Ga_{0.5}N$ (x=50%) for different temperatures.

### 3.1 Acoustic scatterings rates

Acoustic scatterings rates are elastic scatterings which are very important in side valleys. They are characterized by a constant energy. This scattering is very weak in valley Γ; its effects are often shielded by the large number of inter-valley scatterings which are predominant in side valleys. The probability of an acoustic scattering per unit time is given by [17]:

$$\lambda_{ac}(\varepsilon)=\frac{K_B.T.E_{ac}^2.m^{*3/2}}{\rho.S^2.\hbar^4.3\pi.\sqrt{2}}.\delta^{\frac{1}{2}}(\varepsilon).\frac{3(1+\alpha.\varepsilon)^2+(\alpha.\varepsilon)^2}{(1+2.\alpha.\varepsilon)} \tag{4}$$

With: $\delta(\varepsilon)=\varepsilon(1+\alpha.\varepsilon)\,et\,\delta(\varepsilon')=\varepsilon'(1+\alpha.\varepsilon')$

where $K_B$ is the Boltzmann constant, T the temperature of the lattice, $E_{ac}$ an acoustic constant, m* the effective mass of carriers at the bottom of the valley, ρ the density of the material, s the speed of sound, and $\hbar$ Planck's constant.

### 3.2 Piezoelectric scatterings rates

Piezoelectric scatterings rates are scatterings that exist in piezoelectric crystals; they involve an acoustic phonon with a short wavelength. They have a negligible effect on the electrons' behavior because they are elastic and cause no deviation. The probability per unit time of piezoelectric scattering is inversely proportional to the square root of the energy and is given by [18]:

$$\lambda_{pi}=\frac{e^2.K_B.T.P_{pi}^2m^{*1/2}}{4\sqrt{2}\pi.\hbar^2.\varepsilon_0.\varepsilon_S.\delta^{1/2}}.\frac{I}{(1+2a\varepsilon)} \tag{5}$$

With: $I=(1+2\alpha\varepsilon)^2.I\left|\frac{2}{1-\cos a}\right|-2a\varepsilon(1+2a\varepsilon).(1+\cos a)+\frac{(a\varepsilon)^2}{2}.(4-1-\cos a)^2$

$P_{pi}$ is the piezoelectric potential, which has a very small angle (<0.01 radians).

### 3.3 Polar optical scatterings

Polar optical scatterings are very important scatterings in all of the valleys. The phonon energy $\hbar\omega_0$ is comparable to that of electrons at room temperature. Therefore, the phonon temperature cannot be neglected compared with that of electrons and the collisions become inelastic. The probability of scattering per unit time is given by [19] and [20]:

$$\lambda_{op}=\frac{e^2W_{op}m^{*1/2}}{4\sqrt{2}\varepsilon_0\pi\hbar}\left(\frac{1}{\varepsilon_\infty}-\frac{1}{\varepsilon_s}\right)\frac{1+2a\varepsilon}{\delta^{1/2}(\varepsilon)}F(\varepsilon,\varepsilon')\left(N_{op}+\frac{1}{2}\pm\frac{1}{2}\right) \tag{6}$$

Where $F(\varepsilon,\varepsilon')=\frac{1}{c}\left(A.Ln\left|\frac{\delta^{1/2}(\varepsilon)+\delta^{1/2}(\varepsilon')}{\delta^{1/2}(\varepsilon)-\delta^{1/2}(\varepsilon')}\right|+B\right)$

And

$$A = (2(1+\alpha\varepsilon).(1+\alpha\varepsilon') + \alpha(\delta(\varepsilon)+\delta(\varepsilon')))^2$$
$$B = -2\alpha(\delta(\varepsilon).\delta(\varepsilon'))^{1/2}(4.(1+\alpha\varepsilon).(1+\alpha\varepsilon')) + \alpha(\delta(\varepsilon)+\delta(\varepsilon'))$$
$$C = 4((1+\alpha\varepsilon)(1+\alpha\varepsilon')(1+2\alpha\varepsilon)(1+2\alpha\varepsilon')$$

Where $\varepsilon_s$ and $\varepsilon_\infty$ are the relative dielectric permittivities and e is the electron charge.

## 4. RESULTS AND DISCUSSION

### 4.1 Effect of boron content and temperature on the interactions

***A. Piezoelectric scattering rate:***

Figure 1 shows the Piezoelectric scattering rate as a function of energy for the Zinc-blende ternary $B_xGa_{(1-x)}N$ alloy for x=0%, 15%, 35%, 50% , 60%, 80% and 100% boron compositions, at 300 K, with the doping concentration set to $10^{17}$ $cm^{-3}$. We see that the scattering increases with the boron composition. Indeed, the scattering requires little energy, but is highly dependent on the piezoelectric coefficient, which is more important in BN than GaN (Table 2.). This explains the increased probability of these interactions with the addition of boron.

The scattering increases slightly in the upper valleys, with the effective mass of the electrons and rapidly reach saturation (at about 0.5 eV). This agrees well with the theory which predicts that the probability is inversely proportional to the square root of the energy ε.

50% boron incorporation in the GaN material eliminated lattice parameter disagreement, forming a $B_{0.5}Ga_{0.5}N$ alloy. The series of curves presented in Fig. 2 shows the evolution of piezoelectric interactions for the ternary material $B_{0.5}Ga_{0.5}N$ for different temperatures and with a constant electric field $E_z$ = 100 kV / cm. Note that increasing the temperature results in a greater probability for these scatterings. Sometimes, the piezoelectric scattering rate coincides with that resulting from the deformation potential, as in the case of an inter-valley scattering.

***B. Acoustic scattering rate:***

The evolution of this type of scattering as a function of energy, for different boron compositions at T = 300 K, and at a constant electric field $E_z$ = 100 Kv/cm is shown in Fig. 3. These are the most dominant among the elastic scatterings and are mainly caused by the effects of electron doping. For very high temperatures or electric fields, the acoustic scattering becomes predominant. The energy of the electron is greater than that of an optical phonon, so the electron tends to transfer to the network portion of the energy supplied by the electric field. In this ternary material $B_xGa_{(1-x)}N$, the acoustic scatterings, which are proportional to the square of the energy, increase with the boron compositions, since the energy gap and other valleys also increase. Moreover, the difference between the probabilities of the interactions in the lateral valleys L and X increases with increasing boron compositions, because the energy $E_{LX}$ increases with the addition of boron.

Figure 4 shows the evolution of the acoustic scatterings in the ternary material $B_{0.5}Ga_{0.5}N$ for different temperatures at $E_z$ = 100 kV / cm. Note that there is a significant increase in the probability of these scatterings when the temperature increases.

***C. Polar optical scattering rate:***

The polar optical scattering is characterized by a polar optical phonon exchange (energy $\hbar$), and by strong anisotropy in all probable finish states. States corresponding to nearly zero deviation of the wave vector are strongly favored. The electron, which is driven in the direction of the field during the free flight phase, will be diverted from that direction under the effect of this scattering. As can be seen in Fig. 5, the scatterings decrease

Table 2. Piezoelectric coefficient for BN and GaN [21,22].

| Piezoelectric coefficient | e31 | e33 |
|---|---|---|
| BN | 0.27 $cm^{-2}$ | -0.85 $cm^{-2}$ |
| GaN | -0.49 $cm^{-2}$ | 0.73 $cm^{-2}$ |

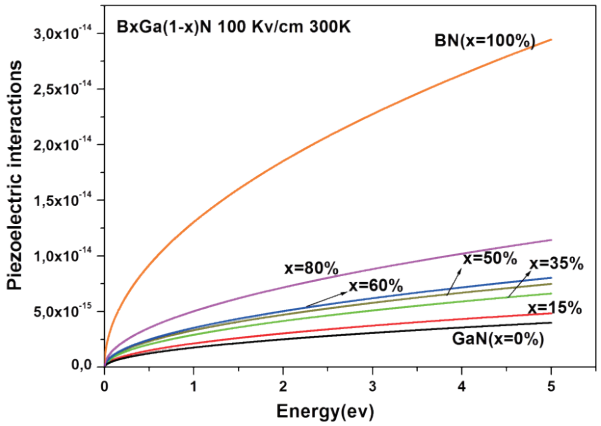


Fig. 1. Piezoelectric scattering rates of $B_xGa_{(1-x)}N$ at 300 K for different boron compositions.

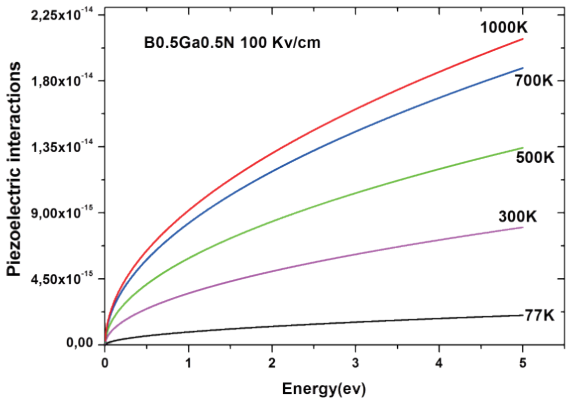


Fig. 2. Piezoelectric scattering rate of $B_{0.5}Ga_{0.5}N$ at different temperatures.

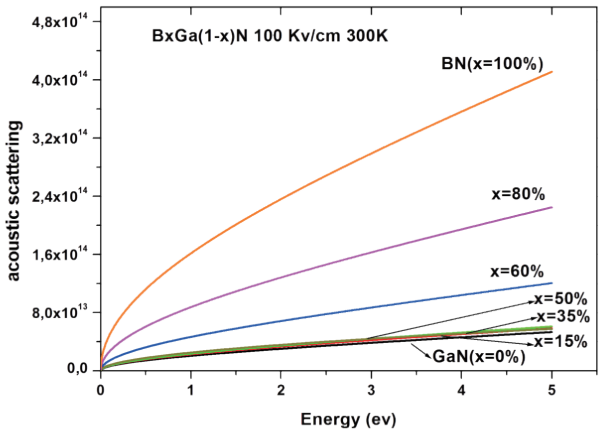


Fig. 3. Acoustic scattering rates of $B_xGa_{(1-x)}N$ at 300 K for different boron compositions.

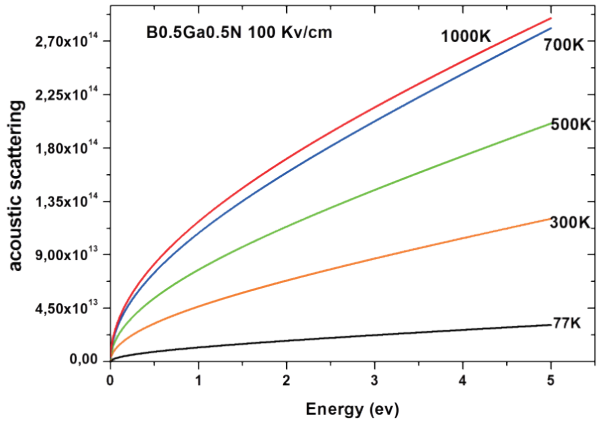


Fig. 4. Acoustic scattering rate of $B_{0.5}Ga_{0.5}N$ at different temperatures.

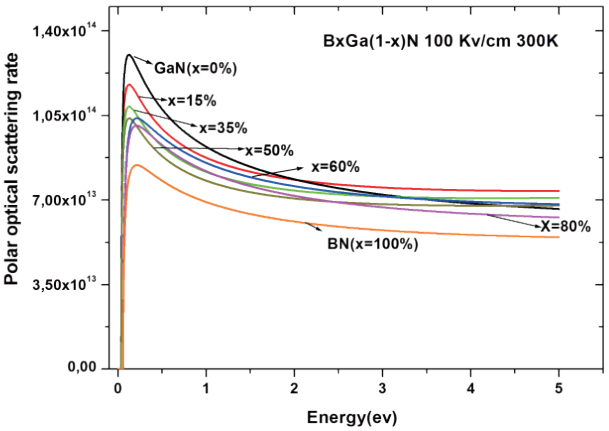


Fig. 5. Polar optical scatterings rates for $B_xGa_{(1-x)}N$ at 300 K for different boron compositions.

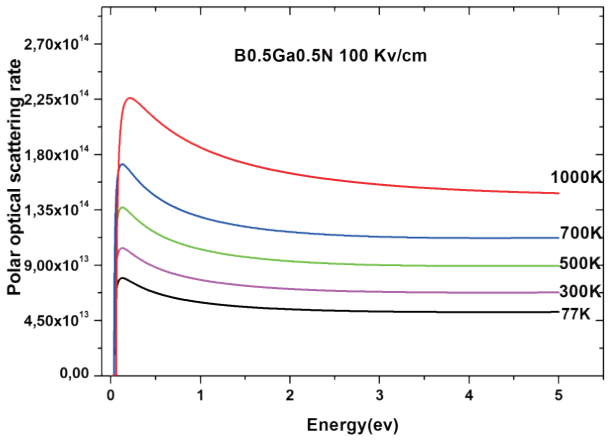


Fig. 6. Polar optical scattering of $B_{0.5}Ga_{0.5}N$ for different temperatures.

while the boron composition increases. Therefore, the electrons will have greater mobility and a longer lifetime. These are desired properties for applications in optoelectronics.

In Fig. 6, we note a slight increase in the probability of the polar optical scattering rates when the temperature increases. The effect of temperature is greater for acoustic and piezoelectric scatterings rates, which means that the scatterings depend greatly on the energy gap.

## 4.2 Effect of boron content and temperature on steady state electron transport

### *A. Electronic energy*

We present in Fig. 7, the average energy for the $B_xGa_{(1-x)}N$ alloy Fig. 5. Polar optical scatterings rates for $B_xGa_{(1-x)}N$ at 300 K for different boron compositions. If we examine the average electron energy as a function of applied electric field, we see that there is a sudden increase, about 100 kV/cm in the case of GaN. Initially, the average energy of the electrons is low, barely higher than the thermal energy, 3/2 $k_BT$ ($k_B$ Boltzmann's constant). The reason for this increase is that the dominant mechanism of energy loss for many III-V compounds including nitrides is due to the interaction of polar optical phonons.

It is observed that by adding boron, the energy gap increases, so it is necessary to apply a stronger electric field. Consequently, the critical electric field becomes larger, reachin 300 kV /cm for BN, but not exceeding 170 kV/cm in GaN. Moreover, the intervalley energy decreases with increasing boron composition, so that the average energy decreases and does not exceed 9×10 eV in the case of BN, while that of GaN is around $3.5\times10^2$ eV.

The electron energy as a function of the applied electric field for different temperatures in $B_{0.5}Ga_{0.5}N$ is shown in Fig. 8. It is noted that the energy is reduced by increasing the temperature due to the small phonon absorption rates at low temperature. Therefore the fractional number of electrons in the Γ valley at low temperature is high.

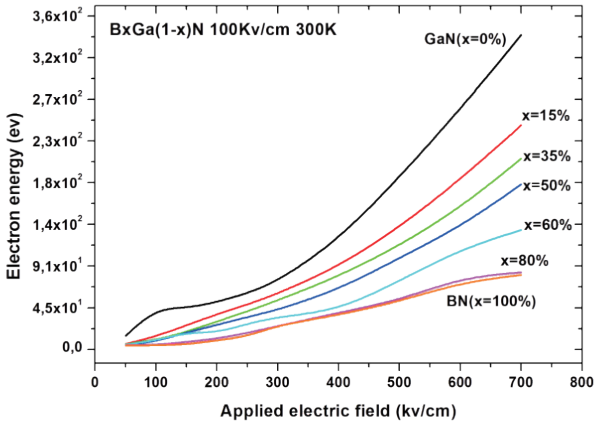


Fig. 7. The electron energy versus the applied electric field of $B_xGa_{(1-x)}N$ alloy for different boron compositions.

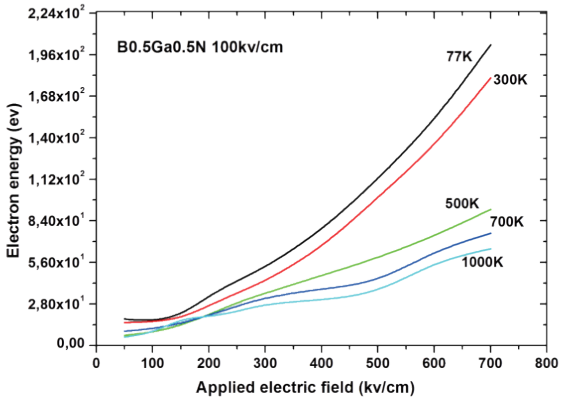


Fig. 8. The electron energy versus the applied electric field of $B_{0.5}Ga_{0.5}N$ alloy for different temperature.

***B. Drift velocity***

The simulated velocity-field characteristics of the Zinc-blende ternary $B_xGa_{(1-x)}N$ alloy for x=0%, 15%, 35%, 50%, 60%, 80%, and 100% boron compositions at 300 K, with the doping concentration set to $10^{17}$ $cm^{-3}$. The electric field applied along one of the cubic axes is presented in Fig. 9.

We see that the curves show the existence of three phases, a rapid and linear increase in the drift velocity with a peak and then the decrease of speed until saturation. The peak drift velocities for BN (X=100%), $B_{0.8}Ga_{0.2}N$ (X=80%), $B_{0.5}Ga_{0.5}N$ (X=50%) and GaN (X=0%) are about $2.42\times10^7$ cm/s, $1.69\times10^7$ cm/s, $1.03\times10^7$ cm/s and $6.8\times10^6$ cm/s at an electric field of about 139.8 kv/cm, 187.7 kv/cm, 95 kv/ cm and $10^9$ kv/cm, respectively. We compared our results with previously published work by F. Nofeli [23] and by Rezaee Rokn-Abadi [24]. The authors used the AlGaN material, which has the same allure. We think the results are in satisfactory agreement. In fact, when the electric field increases above the threshold, the drift velocity decreases. With a high field, the mobility is not constant and varies greatly with the electric field. Beyond a certain critical field, the electrons gain enough energy to transfer to the lateral valleys, which leads to a drop in mobility, then to a saturation velocity of all carriers' vsat. This critical field is greatest in the BN (x=0%) material. In the $B_{0.5}Ga_{0.5}N$ alloy, as in GaN (x=100%), we note that the electron drift velocity increases with the "x" in $B_xGa_{(1-x)}N$ alloy. This effect is, because by increasing the boron composition within $B_xGa_{(1-x)}N$, the energy gap and the effective masse of electrons in the central valley,

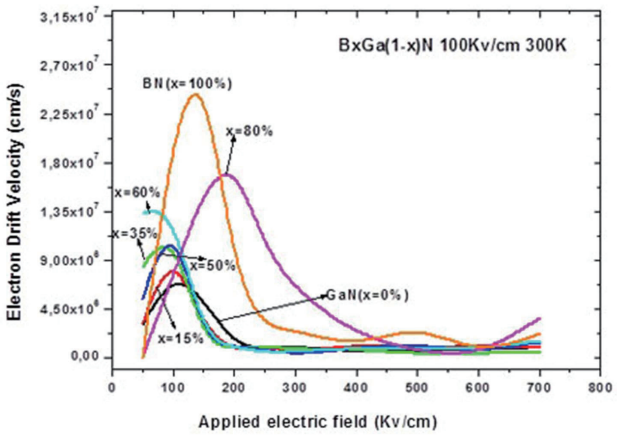


Fig. 9. The electron drift velocity within $B_xGa_{(1-x)}N$ alloy, versus the applied electric field for different boron compositions.

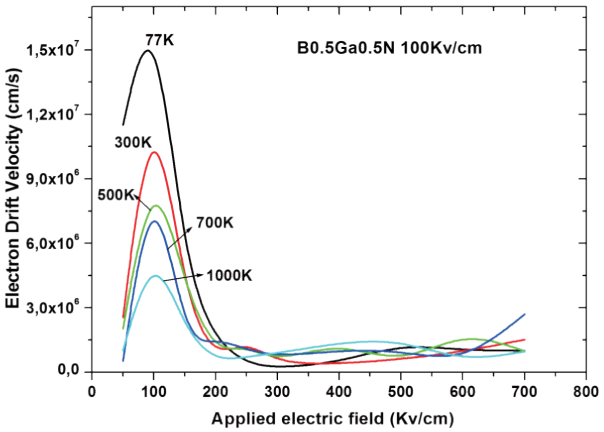


Fig. 10. The electron drift velocity within $B_{0.5}Ga_{0.5}N$ alloy versus the applied electric field for different temperatures.

decrease. This causes an increase in their speed. The energy gap $\Delta E_{rL}$ (transfer of electrons starting from the valley Γ to the valley L) is the most important factor and the probability of interaction with polar optical phonons are higher.

At room temperature, many electrons have higher energy than the energy of polar optical phonons. If we vary the temperature (Fig. 10), the peak of the drift velocity decreases as soon as the temperature increases. This is due to the effect of acoustic scattering, which becomes important as the temperature increases and subsequently increases the lattice vibrations. The increase in temperature results in a decrease in mobility due to interaction with impurities.

## 5. CONCLUSIONS

We have presented the effect of boron content and temperature on interactions and on steady state electron transport in the ternary compound $B_xGa_{(1-x)}N$ for different amounts of boron, using the Monte carlo method to simulate transport phenomena. The obtained results show that the probability of piezoelectric and acoustic scatterings increases with increasing boron compositions and with the temperature whereas the polar optical scattering rate decreases as the boron composition increases. When the electric field increases above the threshold, the velocity decreases, but the velocity increases with increasing boron composition. Finally, we can conclude that the temperature has a greater effect on piezoelectric and acoustic scatterings, which greatly depend on the energy gap. The analysis of the results for the drift velocity of electrons demonstrates the remarkable effect of the boron content in the $B_xGa_{(1-x)}N$ alloy and the applied field on the dynamics of holders within the lattice as a result of interaction mechanisms.

## REFERENCES

[1] S. Nakamura, S. Pearton, and G. Fasol, *Blue Laser Diode* (Springer, Berlin, 1997). [DOI: http://dx.doi.org/10.1007/ 978-3-662-03462-0]

[2] J. Singh, *Electronic and Optoelectronic Properties of Semiconductor Structures* (Cambridge U. Press, County town, 2003). [DOI: http://dx.doi.org/10.1017/CBO9780511805745]

[3] A. Negol, A. Guyot, and J. Zimmermann, *Proc. ASAP 97* (IEEE, Zurich, 1997).

[4] H. Kosina and M. Nedjalkov, *Mathematics and Computers in Simulation* (Elsevier, 2001) p. 55.

[5] B. Bouazza and et al., *Africa Science*, **01**, 55 (2005).

[6] J. Saint Martin, Ph. D. *Thesis*, University of South Paris, France (2005).

[7] J. Pozela and A. Reklaitis, *Solid-St. Electron.*, **23**, 927 (1980).

[8] P. J. Price, *IBM Journal of Research and Development*, **17** (1973). [DOI: http://dx.doi.org/10.1147/rd.171.0039]

[9] R. W. Hockney and J. W. Eastwood, *Computer Simulation Using Paticles* (McGraw-Hill International Book Company, New York, 1981).

[10] C. Jacoboni and P. Lugli, *Springer-Verlag* (1989).

[11] C. Moglestue, *Monte carlo Simulation of Semiconductor Devices* (Chapman & Hall, London, 1993).

[12] L. E Ramos, L. K. Teles, L.M.R. Scolfaro, J.L.P. Castineira, A.L.Rosa, and J. R. Leite, *Phys. Rev. B*, **63**, 165210 (2001). [DOI: http://dx.doi.org/10.1103/PhysRevB.63.165210]

[13] Y. N. Xu and W. Y. Ching, *Phys. Rev. B*, **44**, 7787 (1991). [DOI: http://dx.doi.org/10.1103/PhysRevB.44.7787]

[14] S. V. Ordin, B. N. Sharupin, and M. I. Fedorov, *Smicond.*, **32**, 924(1998).

[15] M. Farahmand, C. Garetto, E. Bellotti, K. F. Brennan, M.

Goano, E. Ghillino, G. Ghione, J. D. Albrecht, and P. P. Ruden, *IEEE Trans. Elect. Dev.*, **48**, 535 (2001). [DOI: http://dx.doi.org/10.1109/16.906448]

[16] V. Bougrov, M. E. Levinshtein, S. L. Rumyantsev, and A. Zubrilov, in: *Properties of Advanced Semiconductor Mate- rials GaN, AlN, InN, BN, SiC, SiGe* (eds. M. E. Levinshtein, S. L. Rumyantsev, and M. S. Shur) (John Wiley & Sons, Inc., New York, 2001) p. 1-30.

[17] C. Moglestue, *Monte carlo Simulation Semiconductor Devices* (CHAPMAN & Hall, New York, 1993). [DOI: http://dx.doi.org/10.1007/978-94-015-8133-2]

[18] C. Hamaguchi, *Basic Semiconductor Physics*, 280 (Springer, 2001).

[19] P. J. Priee, *Phys. Rev. B*, **30**, 2234 (1984).

[20] D. Dolgos, H. Meier, A. Schenk, and B. Witzigmann, *J. Appl. Phys.*, **110**, 084507 (2011). [DOI: http://dx.doi. org/10.1063/1.3652844]

[21] A. F. Wright, *J. Appl. Phys.*, **82**, 2833 (1997). [DOI: http://dx.doi.org/10.1063/1.366114]

[22] K. Kim, W.R.L. Lambrecht, and B. Segall, *Phys. Rev. B*, **53**, 16310 (1996). [DOI: http://dx.doi.org/10.1103/PhysRevB.53.16310]

[23] F. Nofeli, *International Journal of Engineering Research and Applications*, **3**, 2679 (2013).

[24] R. R. Abadi, *M. Indian Journal of Science and Technology*, **3**, (2010).